

Prediction of water erosion sensitive areas in Mediterranean watershed, a case study of Wadi El Maleh in north-west of Algeria

Oussama Benselama  · Mohamed Mazour ·
Mahmoud Hasbaia · Omar Djoukbal ·
Sakher Mokhtari

Received: 6 August 2018 / Accepted: 12 November 2018
© Springer Nature Switzerland AG 2018

Abstract Water erosion phenomenon has significant effects on productivity and environment in Algeria. This contribution presents interesting study on soil erosion risk of Wadi El Maleh watershed using RUSLE model based on original data. The erosion process results from effects of several factors, including rainfall erosivity, soil erodibility, land slope length, land use, and conservation practices. Soil erosion map in the entire watershed area is obtained by the superposition of the generated maps of each previous factor. The obtained results showed that the mean soil loss rate is about 9 t/ha/year in the whole watershed area. These results are comparable to those reported in watersheds having the same hydrologic characteristic. Based on 2017 couples of (Q - C) recorded over 17 years (from 1981 to 1998), we have estimated the suspended sediment transport of Wadi El Maleh to be annually about 2.94 t/ha/year which represents just 32.6% of the eroded rate, i.e., two thirds of the eroded sediment are deposited, especially in the plains. This high values of

deposited sediments is mainly due to relatively moderate slopes and dense vegetation.

Keywords RUSLE · Water erosion · Watershed · Wadi El Maleh · Algeria

Notation Y_w Water yield (m^3)
 Y_s Sediment yield (ton)
 D_{SS} Specific soil degradation ($t/km^2/year$)
 C Suspended sediment concentration (g/l)
 C_v Coefficient of variation
 Q_L Water flow discharge (m^3/s)
 Q_S Sediment discharge (kg/s)
 P Rainfall (mm)
 \bar{P} Average annual rainfall (mm)
 S Surface (km^2)

Introduction

Water erosion is an environmental and agricultural challenge for the most countries, mainly in semi-arid regions. The phenomenon consists of a modification of natural topography due to rainfall intensity and particles cohesion moving from its natural position by destroying the bonds to deposit. It is reported that more than 88% of global soil degradation of which soil erosion is responsible (5.3 t/ha/year of active soils) are transported to lakes and oceans in Africa (Angima et al. 2003). The soil erosion, often spectacularly, is due to the action of various factors which are climate, lithology, nature, soil slope,

O. Benselama (✉) · M. Mazour · O. Djoukbal
Hydraulic Department, LHYDENV Laboratory, University of Ain
Temouchent Belhadj Bouchaib, Ain Temouchent, Algeria
e-mail: benselama.oussama@gmail.com

M. Hasbaia
Hydraulic Department, University of M'sila, 166 Ichebilila,
28000 M'sila, Algeria

S. Mokhtari
Scientific and Technical Research Center on Arid Regions -
Biophysical Environment Station, Touggourt, Algeria

vegetation, and environment. Among those latter, climate is the most important factor, which takes on an aggressive character and causes a rapid degradation of soils when they are not protected by sufficiently dense vegetation (Mazour 1991). In Algeria, about 20 million hectares of lands are affected by erosion, particularly in mountainous areas where 90% of dams are implanted and about 20 million of people are concentrated (Mazour and Roose 2002). The Agriculture Ministry (MADR 2011) recorded that 50 million hectares of land are threatened by degradation due to desertification and water erosion which represents about 20% of the total surface of Algeria and that includes 14 million hectares of mountain areas in the north part of the country suffer from water erosion.

These high rates are a serious problem not only for Algeria, but is also reported by many other countries or continents. For instance, soil degradation rates varies between 19 and 39 t/ha/year in Asia, Africa, and South America and is less pronounced as in Europe where it ranges between 10 and 20 t/ha/year (Warwade et al. 2014).

Our literature survey reveals that many approaches were used to diagnose and analyze soil loss. It is worth noting the Universal Soil Loss Equation USLE (Wischmeier and Smith 1965, 1978), its modified version MUSLE (Williams 1975; Williams and Berndt 1977), its revised version RUSLE (McCool et al. 1995), and its improved version RUSLE2 (Foster et al. 2003).

The RUSLE model has been applied extensively worldwide in several watersheds for estimating soil erosion under GIS environment and remote sensing, in Algeria (Toumi et al. 2013; Hasbaia et al. 2017; Benchettouh et al. 2017; Bouguerra et al. 2017; Toubal et al. 2018; Djoukbala et al. 2018), in Morocco (Tahiri et al. 2016; Chadli 2016), in Spain (Fernández and Vega 2016), in Greece (Karamesouti et al. 2016), in Italy (Siciliano 2009), in Turkey (Ozsoy and Aksoy 2015), in India (Markose and Jayappa 2016; Rejani et al. 2016), in Portugal (Duarte et al. 2016), and in Himalayas (Semwal et al. 2017). In this paper, we aim to use RUSLE approach to map the soil loss in a coastal watershed in north-west region of Algeria. Wadi El Maleh presents a typical case of the watersheds of this region with the advantage of the data availability required by RUSLE model, especially, the

sediment transport data recorded from the Turgot Nord gauging station, situated at the outlet of the basin.

Material and methods

Study area

As it is shown in Fig. 1, Wadi El Maleh watershed drains a surface of 932.56 km² with a perimeter of 194.8 km (Table 1), situated in Ain Temouchent Department, in north-west of Algeria. It is located between 1° 9' 24" and 1° 26' 17" W of longitude and between 35° 17' 22" and 35° 16' 37" N of latitude. Its climate is typically Mediterranean semi-arid. The relief of Wadi El Maleh decreases from south to north, which the altitudes vary from 808 at the summit to 0 at the outlet. The annual rainfall (P) is very irregular, varying from 241 mm/year to 616 mm/year and the inter-annual average rainfall \bar{P} is about 382.68 mm associated with a variability (inter-annual coefficient of variation $C_v = 28\%$) during 43 years. The maximum temperature in the watershed varies from 20 to 26.9 °C, in the same way, for the minimal temperature, they range from 11.9 and 16.4 °C.

RUSLE model

RUSLE equation is an empirical model that has been used to evaluate the soil loss at watershed scale. McCool et al. 1995 proposed the same formula with improvements considering many erosion factors that led to a different approach to estimate erodibility K , a method for the topographic factor LS , a new value for crop management factor C and anti-erosive practices factor P .

The application of the RUSLE model requires the examination of various parameters involved in the erosive processes and their spatialization in thematic maps. Its development for each RUSLE factor, under GIS techniques facilitates their superposition and their treatment. This approach is much more used in agricultural than in forest environments to estimate the rate of sheet erosion. The RUSLE equation is expressed by the following formula:

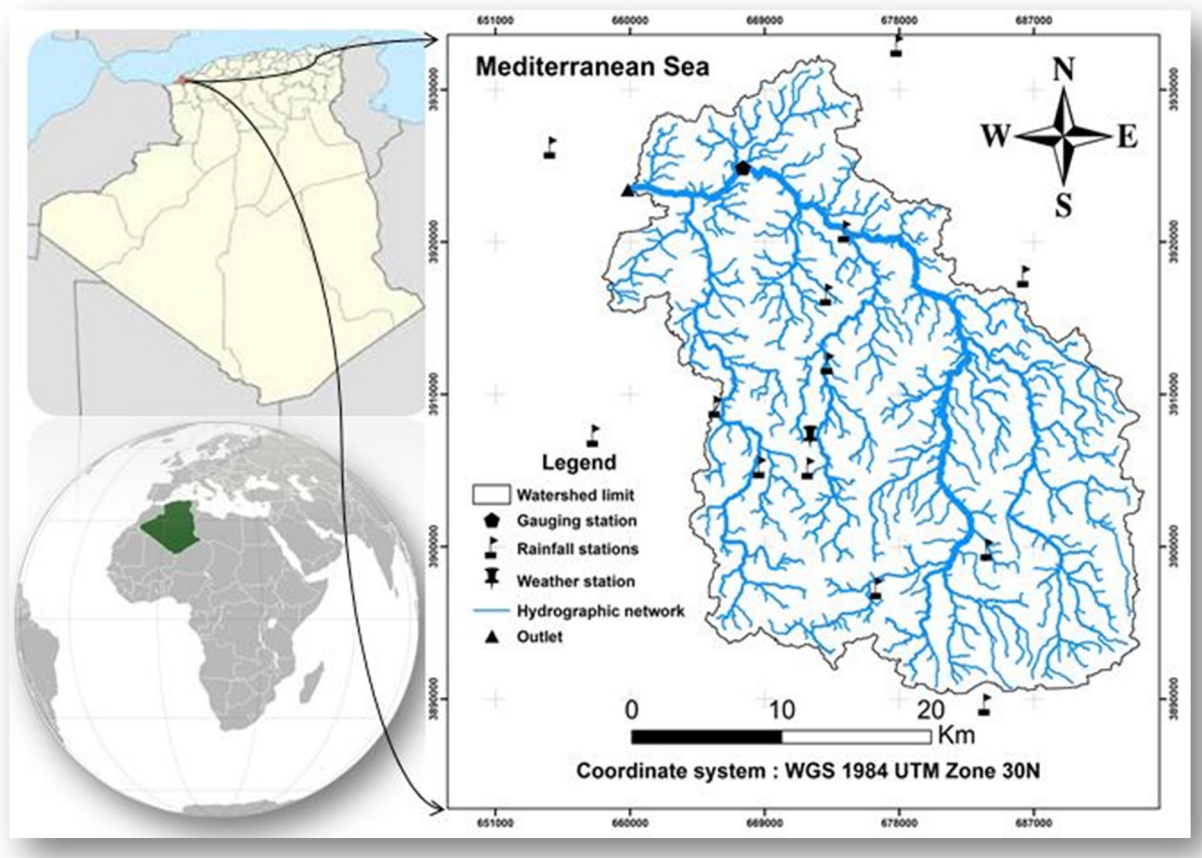


Fig. 1 Location of Wadi El Maleh watershed

$$A = R \times K \times LS \times C \times P \tag{1}$$

where

- A* Soil loss (t/ha/year);
- R* Climatic aggressiveness parameter (MJ mm/ha/h/year)
- K* Soil erodibility parameter (Mg h/MJ/mm)
- LS* Topographic parameter (Unit-less)
- C* Crop management parameter (Unit-less)
- P* Anti-erosive practice parameter (Unit-less)

Rainfall erosivity index (*R*)

The rainfall erosivity *R* in the RUSLE model is defined as a long-term average of kinetic energy. This factor is obtained from the kinetic energy of raindrops *E* in a short time interval, i.e., 30 min which expresses the effect of runoff. The erosivity factor is calculated from downpours exceeding 12.7 mm (Wischmeier and Smith 1978). It is the

energy of the raindrops that sets of the process of aggregate destruction while the runoff ensures their transport (Roose and Lelong 1976). The erosivity *R* is estimated by the formula (Wischmeier and Smith 1978) as

$$R = MEc I_{30} \tag{2}$$

where

- M* A coefficient dependent on the system of measurement units
- E_c* The kinetic energy of the 30-min intensity (*I₃₀*) of the raindrops of every storm

In this study, we cannot use the previous formula due to the lack of rainfall intensity data, indeed, it is the same case of the majority of Algerian watersheds. The best reliable rainfall data are recorded at the daily, monthly, and annual scales; for this reason, we have preferred to use an alternative equation based on monthly and annual rainfall (Eq. 3). This formula was proposed and used by many researchers (Kalman 1967; Arnoldus 1980;

Table 1 Hydro-morphometric characteristics of Wadi El Maleh watershed

Parameters	Notation	Unit	Values
Area	S	km ²	932.56
Perimeter	P	km	194.8
Circularity ratio	K _c	–	1.78
Maximum altitude	H _{max}	m	808
Minimum altitude	H _{min}	m	0
Average altitude	H _{moy}	m	283.11
Length of equivalent rectangle	L _{rec}	km	86.27
Width of equivalent rectangle	l _{rec}	km	10.81
Length of the main stream	L	km	67.4
Average slope of the main stream	I _{cp}	%	11.99
Time of concentration	T _c	h	16.59
Global slope index	I _g	%	0.67
Roche slope index	I _p	%	2.85
Drainage density	D _d	km km ⁻²	1.21
Hydrographic density	F	km km ⁻²	2.27
Streams frequency	Fr	km ⁻¹	1.18

Rango and Arnoldus 1987; Sadiki et al. 2004; Djoukbal et al. 2018):

$$\log R = 1.74 \log \sum_{i=1}^{12} \frac{P_i^2}{P} + 1.29 \quad (3)$$

where

R Rainfall erosivity factor (MJ mm/ha h year)

P_i Monthly rainfall (mm)

P Annual rainfall (mm)

Erodibility factor (*K*)

Soil erodibility factor *K* is a risk parameter that affects erosion processes by measuring soil contribution (Kumar and Gupta 2016). Soils differ according to erosion resistance, depending on texture, structure, roughness, organic content, and degree of soil moisture.

The soil resistance is lower when the soil is shallow and higher for deeper soils. When the surface soils are however saturated, there is a movement of particles on the slope even for very low values as stated by (Ryan 1982). In this study, soil map of the world called The Harmonized World Soil Database (HWSD) is used to determine the *K* factor (Fao and Rome 2012). This latter provides many information on soil parameters

worldwide as it allows an estimate potential land productivity, helps identify land and water boundaries, and improve assessment of land degradation risks, particularly soil erosion.

The HWSD is a 30-arc-s raster database with over 16,000 different soil mapping units that combines existing regional and national updates of soil information worldwide.

The raster database consists of 21,600 rows and 43,200 columns, with 221 million grid cells covering the globe's land territory which are linked to harmonized soil property data. The use of a standardized structure allows for the linkage of the attribute data with the raster map to display or query the composition in terms of soil units and the characterization of selected soil parameters (organic carbon, pH, water storage capacity, soil depth, cation exchange capacity of the soil and the clay fraction, total exchangeable nutrients, lime and gypsum contents, sodium exchange percentage, salinity, textural class, and granulometry). The *K* factor was calculated using the following formulas proposed and used by (Wawer et al. 2005; Neitsch et al. 2011; Anache et al. 2015; Chadli 2016; Djoukbal et al. 2018).

$$K = E_{\text{sand}} \cdot E_s \cdot E_{Oc} \cdot E_{\text{topsand}} \quad (4)$$

where

E_{sand} Is parameter that lowers the indicator *K* in soils that contains coarse sand

E_z Indicate low soil erodibility parameter for lands with high clay

E_{Oc} Curb *K* values in soils that contains organic carbon

E_{topsand} Reduces *K* values for soils with very high sand content

$$E_{\text{sand}} = \left(0.2 + 0.3 \cdot \exp \left[-0.256 \cdot p_s \cdot \left(1 - \frac{P_{\text{silt}}}{100} \right) \right] \right) \quad (5)$$

$$E_s = \left(\frac{P_{\text{silt}}}{p_c + P_{\text{silt}}} \right) \quad (6)$$

$$E_{Oc} = \left(1 - \frac{0.25 \cdot Oc}{Oc + \exp[3.72 - 2.95 \cdot Oc]} \right) \quad (7)$$

$$E_{\text{topsand}} = \left(1 - \frac{0.7 \cdot \left(1 - \frac{P_s}{100} \right)}{\left(1 - \frac{P_s}{100} \right) + \exp \left[-5.51 + 22.9 \cdot \left(1 - \frac{P_s}{100} \right) \right]} \right) \quad (8)$$

where

- P_s The percent sand
- P_{silt} The percent of silt
- P_c The percent of clay
- O_c The percent of organic carbon

Land use parameter (C)

Land cover and vegetation are related to topography, geology, soils, climate, and features hydrological. Land cover is linking to human activities, agriculture, live-stock, mining, and forestry; urbanization have a strong influence on erosion (White 1986).

C parameter is a conservation linked factor. In most cases, values close to 0 are attributed to areas with a high vegetation cover, while those close to 1 correspond to bare lands (Semwal et al. 2017).

In the reported above study, the values of this parameter are estimated by the normalized difference vegetation index ($NDVI$). The $NDVI$ is a mathematical formula (Eq. 8) expressing the difference between reflectance in the red band (R) and near infrared band (NIB) portion of the electromagnetic spectrum. This index is linked to the nature of the vegetation and its percentage. This remote sensing indicator was calculated from a combination of *Landsat TM8* of the year 2018 with a resolution of 30 m. The formula used is:

$$NDVI = \frac{NIB - R}{NIB + R} \quad (9)$$

where

- NIB Near infrared band
- R Red band

The classification of vegetation is carried out according to the following thresholding conditions:

- $NDVI < -0.1$: Water;
- $-0.1 < NDVI < 0.15$: Bare ground;
- $0.15 < NDVI < 0.25$: Sparse vegetation;
- $0.25 < NDVI < 0.4$: Medium density vegetation;
- $NDVI > 0.4$: Dense vegetation.

The maximum $NDVI$ value reflects upmost percentage of vegetation cover and also represents the good

condition of the vegetation. Areas without vegetation (bare soil and water bodies) have a low $NDVI$ value. Gitas et al. (2009), Toumi et al. (2013), and Djoukbal et al. (2018) have used this equation to calculate the C parameter from:

$$C = 0.9167 - 1.1667 \times NDVI \quad (10)$$

Slope length index (LS)

The steep slopes with a fast flow are generally the cause of a significant erosion whose importance depends on the geology, the soil nature, and the vegetal cover; the higher the slope, the more the runoff will erode the soil. For this reason, a digital elevation model (DEM) of the area is obtained from the ASTER GDEM (Advanced Spaceborne Thermal Emission and Reflection Radiometer Global Digital Elevation Model) downloaded from the Earth Explorer platform of the United States Geological Survey (USGS) accessed on 2018. In the present study, we used the formula developed by Wischmeier and Smith (1978)) and also used by many authors (Vezena and Bonn 2006; Khosrowpanah et al. 2007; Toumi et al. 2013; Djoukbal et al. 2018).

$$LS = \left(\frac{L}{22.13} \right)^A (0.06G + 0.045G + 0.065G^2) \quad (11)$$

where :

- L The slope length (m)
- G The angle of the slope
- A Parameter where: $a = 0.5$ if $S > 5\%$, $a = 0.4$ if S equal between 3.6 and 4.6%, $a = 0.3$ if S varies between 1 and 3%, and $a = 0.2$ if $S < 1\%$

The both factors L and G can be estimated separately from DEM . For the slope length, the technique consists in determining the delimitation of the watersheds where the flow encounters no obstacle.

Agricultural practices and soil conservation factor (P)

This factor P is dimensionless and incorporates anti-erosion cultural techniques; namely, bypassed crops, alternating strips or terraces, and reforestation in banquettes. It reflects the effects of practices that reduce the amount of runoff and their rate and the effects of water erosion. The values of this factor P are between 0 and

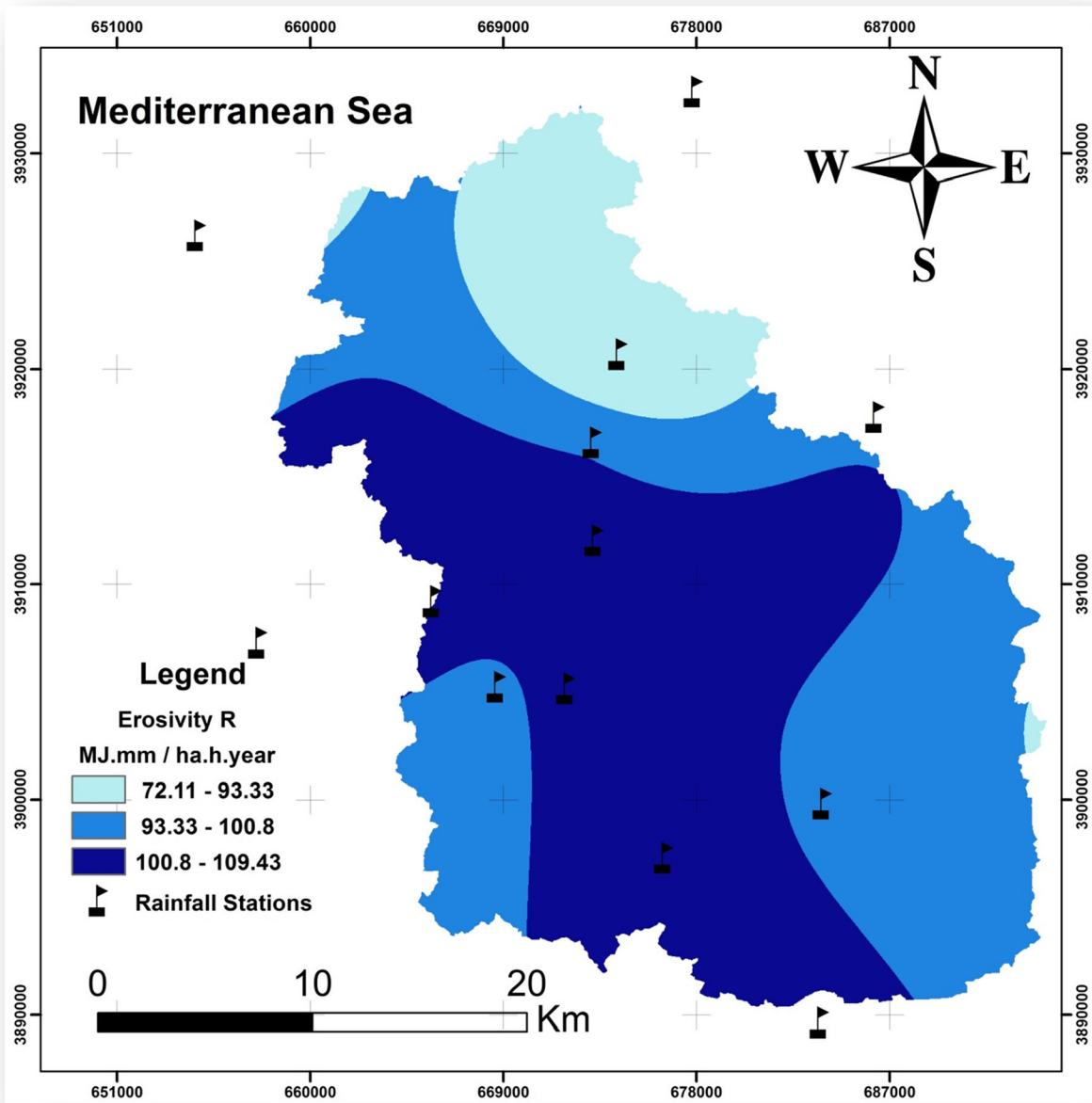


Fig. 2 Spatial distribution of *R* factor values in Wadi El Maleh watershed

1. The value 0 indicates that the soil is very tough to the loss of human origin, while, the value 1 is due to the absence anti-erosive practices.

Estimating of suspended sediment transport from gauging station data

We have in this part estimated the suspended sediment transport using the instantaneous data of water flow discharge Q_L and sediment discharge Q_S , measured in

Table 2 Distribution of *R* factor classes in Wadi El Maleh Watershed

Classes of <i>R</i> factor	Area (km ²)	Area (%)
72.12 – 93.33	142.5	15.29
93.33 – 100.8	412.97	44.31
100.8 – 109.43	375.41	40.28

Table 3 Estimation of *K* factor in Wadi El Maleh watershed

Soil samples	Sand topsoil (%)	Silt topsoil (%)	Clay topsoil (%)	Organic carbon (%)	E_{sand}	E_s	E_{Oc}	$E_{topsoil}$	<i>K</i> values
S1	48.7	29.9	21.6	0.64	0.21	0.85	0.98	1.01	0.0218
S2	58.9	16.2	24.9	0.97	0.21	0.76	0.93	0.99	0.0183
S3	47.8	8.5	43.8	0.38	0.21	0.58	0.99	1.01	0.0151
S4	49	10.7	40.3	0.13	0.21	0.63	1.00	1.01	0.0164
S5	63.5	17.9	18.7	0.26	0.21	0.81	1.00	0.99	0.0208
S6	63.5	19.2	17.3	0.76	0.21	0.82	0.96	0.99	0.0226

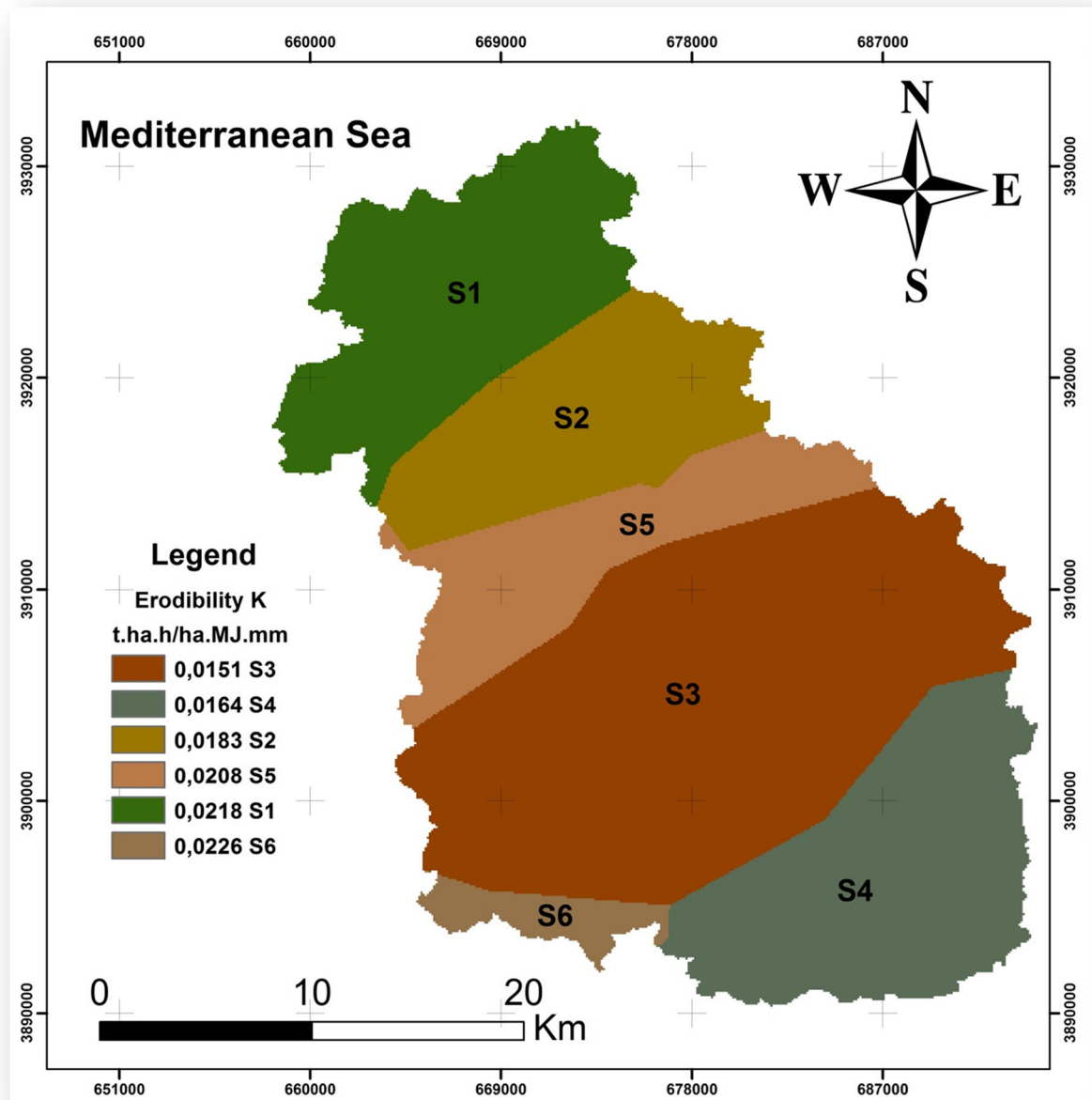


Fig. 3 Spatial distribution of *K* factor values in Wadi El Maleh watershed

gauging station, these data are the number of 2017, recorded over a period of 17 years (1981–1998).

The annual sediment yield transported during a time interval $(t_{i+1} - t_i)$ is calculated by the formula:

$$Y_S = \frac{(Q_{Li+1}C_{i+1}) + (Q_{Li}C_i)}{2}(t_{i+1}-t_i) \quad (12)$$

where C_i and C_{i+1} are the concentrations observed at instants t_i and t_{i+1} ; respectively corresponding to the water flow discharge Q_{Li} and Q_{Li+1} .

Table 4 Distribution of K factor classes in Wadi El Maleh watershed

K	Area (km ²)	Area (%)
0.0226	32.01	3.43
0.0151	348.16	37.33
0.0183	121.72	13.05
0.0208	105.2	11.28
0.0164	162.85	17.46
0.0218	162.6	17.44

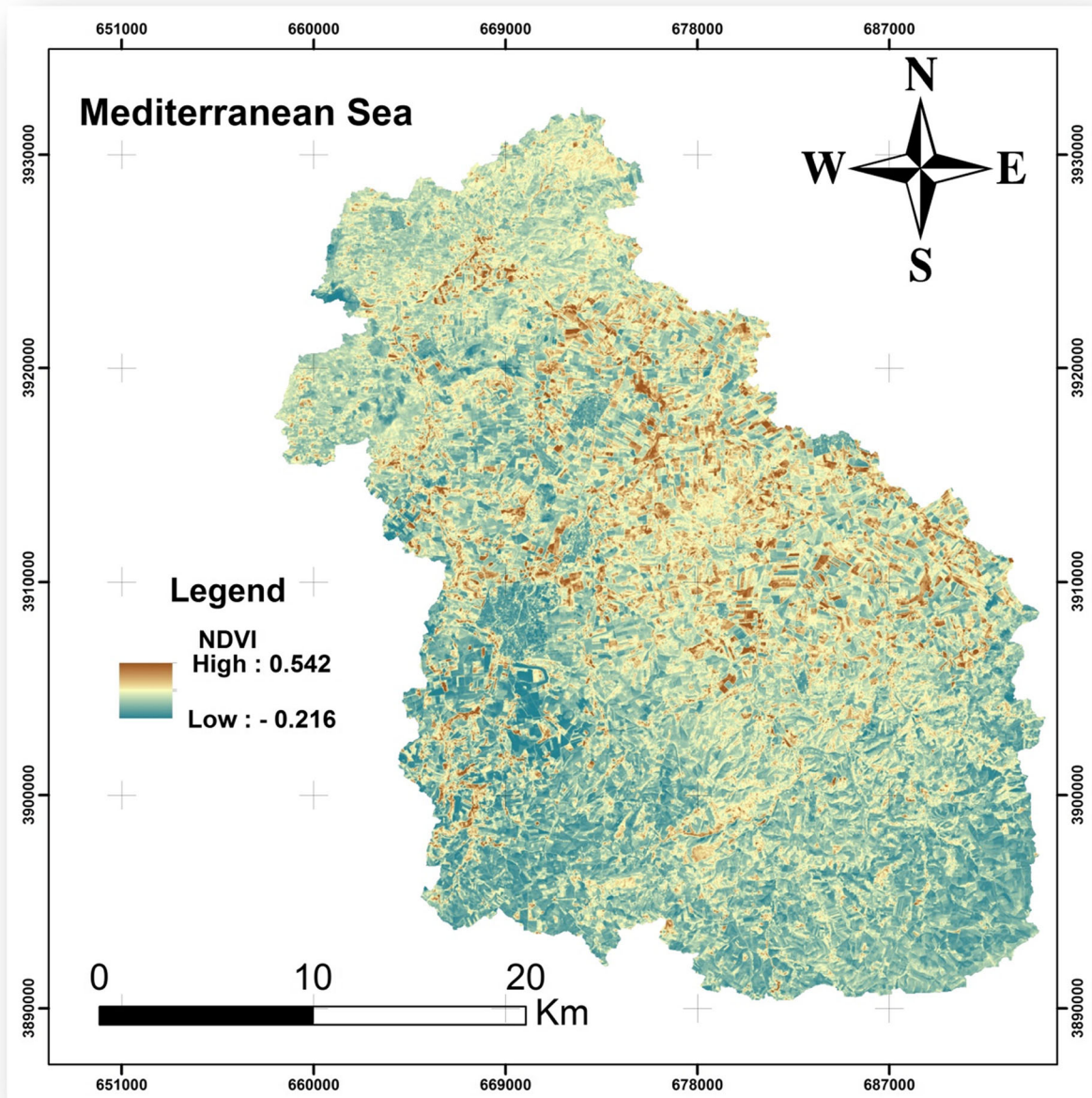


Fig. 4 Spatial distribution of $NDVI$ index values in Wadi El Maleh watershed

Table 5 Distribution of *NDVI* index classes in Wadi El Maleh watershed

Classes of <i>NDVI</i> index	Area (km ²)	Area (%)
-0.21 – 0.1	230.25	25.05
0.1 – 0.18	364.45	39.65
0.18 – 0.54	502.91	35.31

The arithmetic sum of these elementary contributions during the year will constitute the annual sediment yield. Similarly, the water yield is calculated as follows:

$$Y_w = \frac{Q_{Li+1} + Q_{Li}}{2} (t_{i+1} - t_i) \tag{13}$$

The specific soil erosion is calculated by dividing the annual sediment yield Y_s [t/year] by the area of the watershed S [km²] according to the following formula:

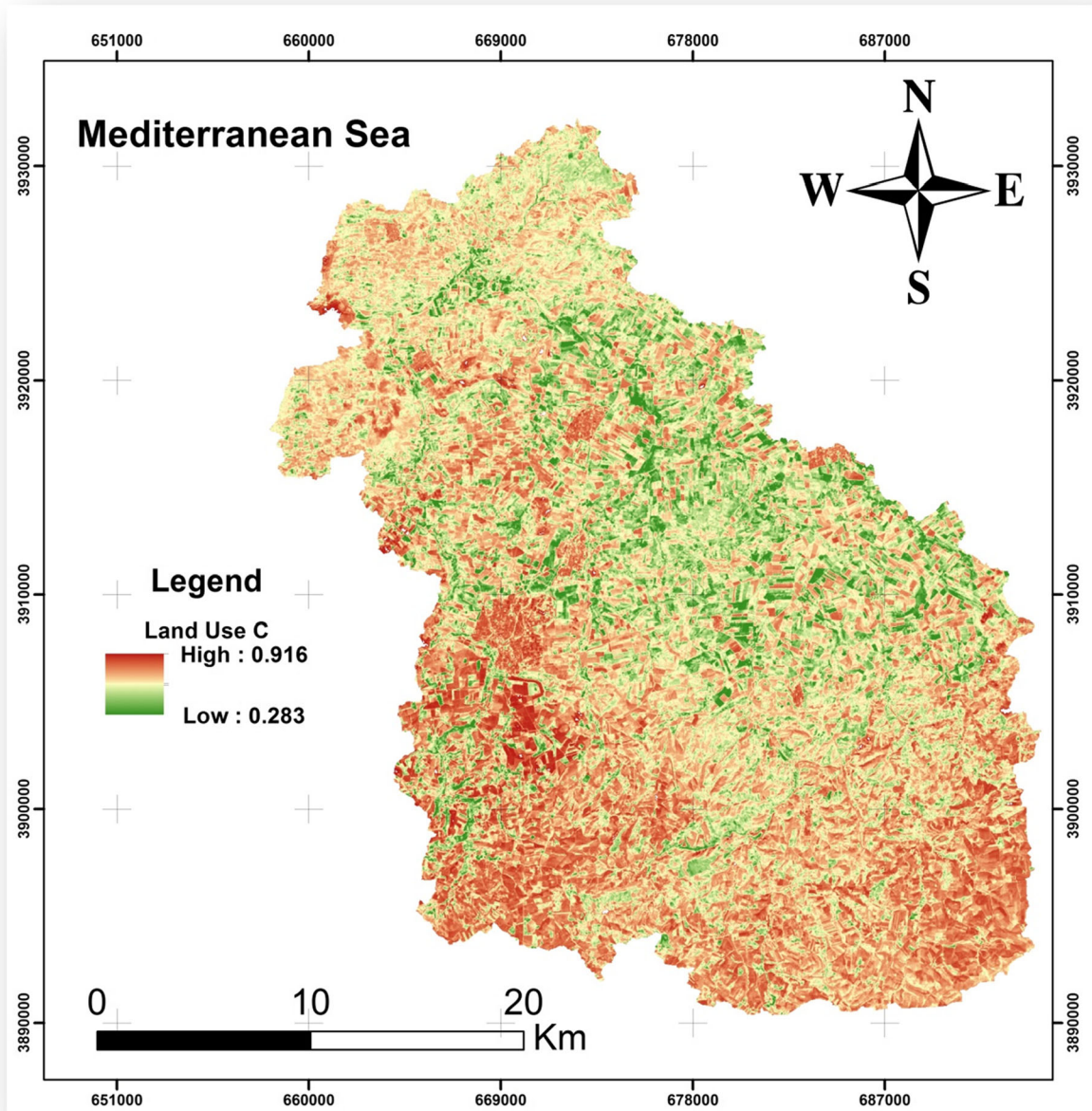


Fig. 5 Spatial distribution of *C* factor values in Wadi El Maleh watershed

Table 6 Distribution of *C* factor classes in Wadi El Maleh watershed

Classes of <i>C</i> factor	Area (km ²)	Area (%)
0.28 – 0.64	152.41	16.35
0.64 – 0.75	399.32	42.85
0.75 – 0.91	380.27	40.81

$$D_{SS} = Y_S/S \quad (14)$$

Results and discussion

Estimating of the RUSLE factors

Rainfall erosivity (*R*)

As displayed in Fig. 2, Wadi El Maleh watershed has a dense weather network with 13 rainfall stations, nine of them are within the watershed and the others are neighboring.

The used rainfall data have different measurement periods, ranging from 25 to 76 years. The erosivity index is calculated and interpolated using a geostatistic model. In Fig. 2, the obtained rainfall-runoff map of Wadi El Maleh watershed shows that the *R* values vary between 72.11 and 109.43 MJ.mm/ha h year with an average of 99.28 MJ mm/ha h year. The lowest *R* values presented by the class (72.11 to 93.33 MJ mm/ha h year) with more than 15% mostly focus in northeast of the catchment, while the highest values over 100.8 MJ mm/ha h year focus in the center of the watershed. The major class of *R* value distribution between 93.33 and 109.43 represents 84% of the total surface (Table 2). The rainfall aggressiveness is experiencing an increasing gradient from the north of

Table 7 Distribution of *LS* factor class in Wadi El Maleh watershed

Classes of <i>LS</i> factor	Area (km ²)	Area (%)
0 – 3	367.80	39.55
3 – 6	213.56	22.96
6 – 9	162.87	17.51
9 – 18	106.95	11.50
18 – 42.5	78.83	8.48

the area to the south. Wadi El Maleh watershed is under a high climatic aggressiveness.

Soil erodibility (*K*)

We have estimated the soil erodibility *K* factor In Wadi El Maleh watershed. This factor has an average value of 0.0191 t ha h/ha MJ mm. As summarized in Table 3, the *K* factor values range from 0.0151 to 0.0226. Clay and sandy soils have low *K* values since they are resistant to detachment and have a high infiltration rate and thus reduced runoff. Moderate *K* values were observed with loamy clay soils for which long particles are easy to remove.

It is reported that the variation in the rate of soil loss depends on the types of soils, the time scale and the nature of the cultivation techniques (Elaloui et al. 2017). The results presented in Fig. 3 and Table 4 showed that the high erodibility zone represents 37.33% of the total watershed's area and it is located in the south of the watershed. This high value is due to coarse nature of soils that favor infiltration. High *K* values indicates that land degradation is susceptible to occur. The erodibility map (Fig. 3) shows the spatial distribution of soil erodibility over the whole Wadi El Maleh watershed.

Land use (*C*)

As indicated in Fig. 4, the *NDVI* values vary between – 0.21 and 0.54, with an average of 0.16 (Table 5). More than 64% is located in the southern part of the watershed, these low values show bare ground and water bodies, while, about 33% of *NDVI* values are concentrated in the center of the watershed, these high values are variable vegetation lands.

Figure 5 shows the obtained map of the *C* factor in which the values vary from 0.283 to 0.916. More than 84% of the watershed's surface is characterized by *C* factor values greater than 0.64 (Table 6), observed in the regions located mainly in the south. These areas are islands of bare or fallow soils. However, values ranging from 0.28 to 0.64, representing more than 16% of the total surface, are in general attributed to areas are covered with cereal and forage crops. These results confirmed that bare areas are more affected by erosion and soil loss, while areas with a vegetal cover are the most resistant to this phenomenon.

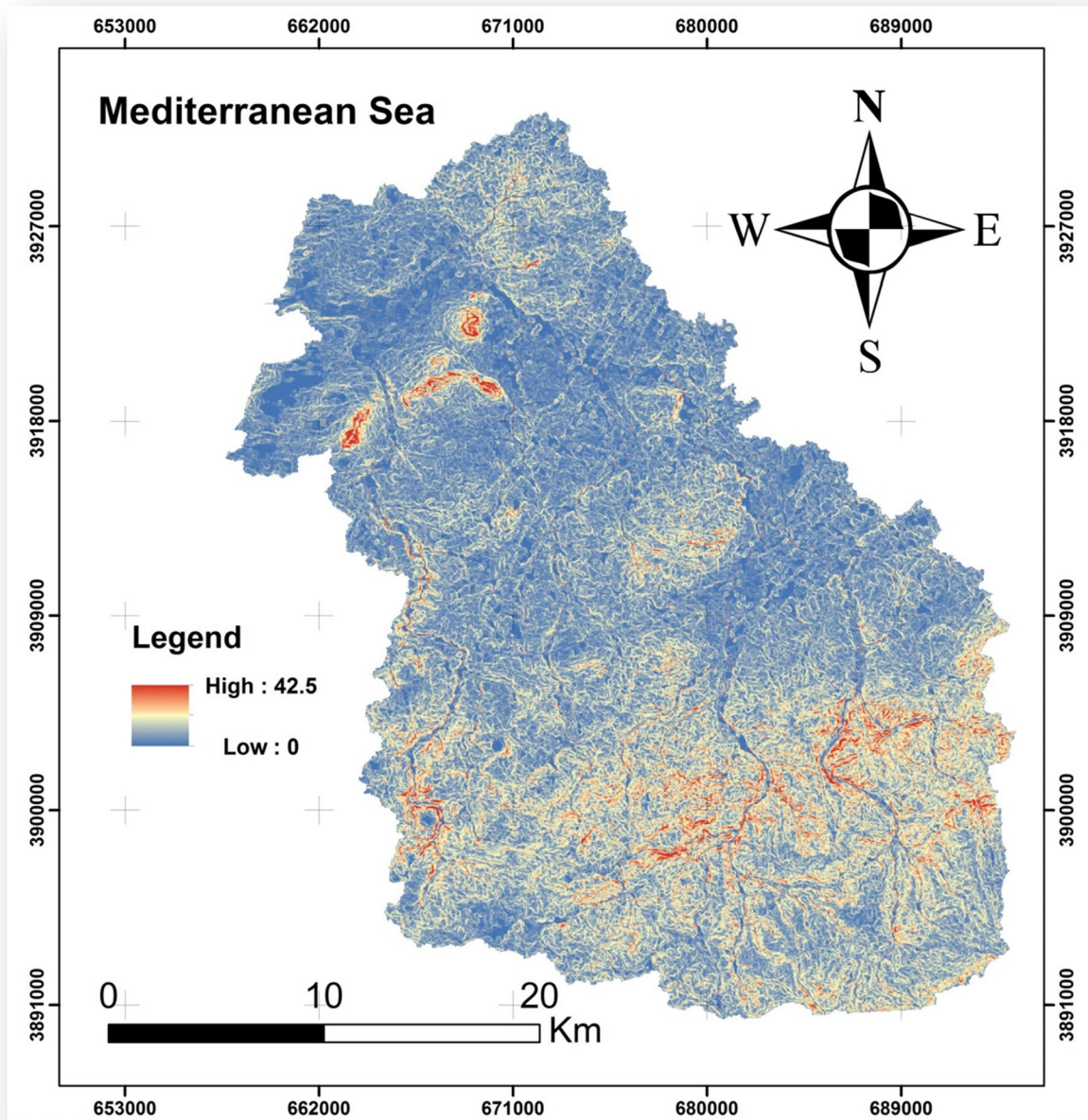


Fig. 6 Spatial distribution of *LS* factor values in Wadi El Maleh watershed

Topographic factor (LS)

As far as the *LS* factor is concerned, high values are more vulnerable to erosion. At Wadi El Maleh watershed, *LS* has a mean value of 5.38 with variability ranging from 0 to 42.5 and classified into five classes as represented in Table 7.

The length and degree of inclination of the slope were decisive factors in the erosion process. The

obtained *LS* factor map perfectly reflects the topography of the watershed as shown in (Fig. 6). The values of less than 6 occupy 62.51% of the surface of Wadi El Maleh catchment, corresponding to low lying areas. Values greater than 6 (37.49%), indicate rugged terrain with a steep slopes. This parameter presents an erosion risk factor according to the slope zones at the watershed scale, more than this factor is high, more than the watershed is eroded.

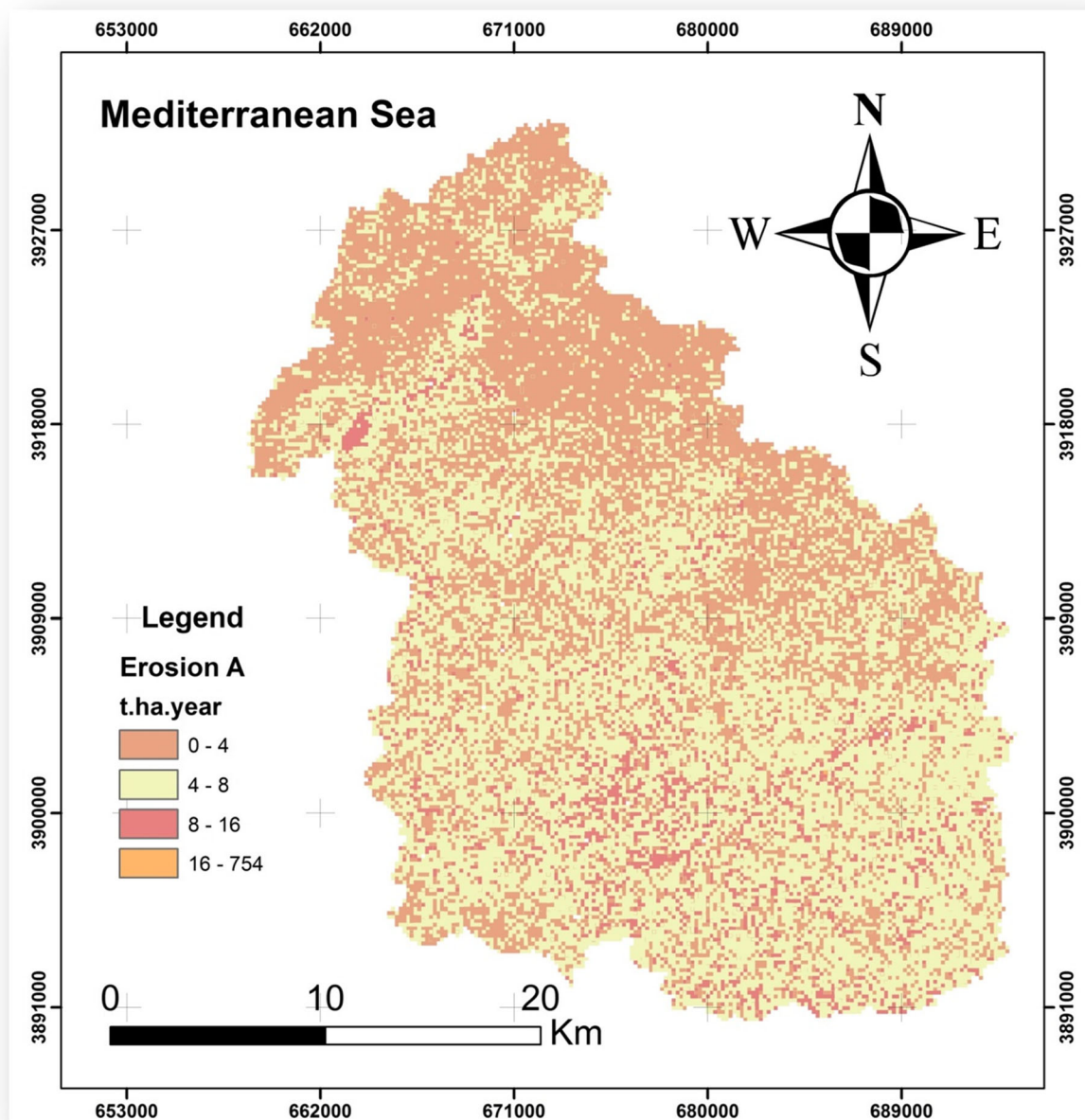


Fig. 7 Soil erosion map A of Wadi El Maleh watershed

Soil conservation support practice factor (P)

In the whole Wadi El Maleh watershed, there are no important conservation structures and farmers are not using soil conservation practices. Crops are mainly cereal, and plowing is rarely parallel to contour lines. According to Ganasri and Ramesh 2016, the soil conservation factor P varies from 0 for good practices anti-erosive to 1 for poor practices. In this particular situation, the value of 1 is assigned to the P factor in the entire watershed area.

Potential erosion risk map (A)

The multiplicative superposition of the four thematic layers generates the soil erosion map in Raster format, expressing the potential erosion in t/ha/year per spatial unit.

The obtained map (Fig. 7) shows that the erosion rates have a wide range of values, they vary from 0 to 754 t/ha/year over the entire study area with an average around 9 t/ha/year.

Table 8 Distribution of soil loss A classes in Wadi El Maleh watershed

Classes of A soil loss	Area (km ²)	Area (%)
0 – 4	398.04	42.81
4 – 8	247.38	26.22
8 – 16	273.42	29.42
16 – 754	11.12	1.22

According to Wall et al. 2002, very low to low erosion varies between 0 and 11 t/ha/year, moderate erosion is between 11 and 22 t/ha/year while for high erosion, the values vary between 22 and 33 t/ha/year; values above 33 t/ha/year correspond to very high erosion.

In this study, the soil loss map has been classified into four classes for a better spatial visualization of soil losses (Fig. 7; Table 8).

The first class concerns the areas which soil loss is less than 4 t/ha/year. Nearly half of Wadi El Maleh watershed has low water erosion (between 0 and 4 t/ha/year), which represents 42.8% of the watershed’s surface, mainly concentrated in the north of the watershed. While, more than 55% of the total surface has an important water erosion and the soil is less protected.

This finding agrees with that observed in many watersheds of Algeria, especially in the northwest region, such as in Wadi Mina watershed at 11.2 t/ha/year and in Wadi Boumahdane of 11.18 t/ha/year (Benchettouh et al. 2017; Bouguerra et al. 2017) respectively.

The specific soil erosion calculated from gauging station data

Using the measured data in gauging station, we conclude that Wadi El Maleh watershed with an area of 932.56 km² losses annually 2.94 t/ha/year, equivalent to

Table 9 Flood characteristic of January 1988

Flood	Values
Water discharge peak (m ³ /s)	54.6
Maximum concentration (g/l)	147.3
Water yield of flood (Mm ³)	13.55
% of water yield of flood/annual water yield	55.18
Sediment yield of flood (Mt)	0.823
% of sediment yield of food/annual sediment yield	92.95

an average of 23 million m³ of water yield per year, with a high variability ($C_v = 65\%$) and 274,000 tons of sediment, with a very high variability ($C_v = 125\%$). The results are also compatible with other studies carried out in watersheds having a similar climatic and environmental characteristics. In north-west region of Algeria, similar values are observed in Wadi Mina (2.11 t/h/year) and in Wadi Haddad (2.12 t/ha/year) (Hallouz et al. 2017; Achite and Meddi 2004) respectively. The major part of the suspended sediment transport in Wadi El Maleh watershed occurs mainly during extreme events. The runoff transports on average more than 64% in the total sediment yields during floods. This percentage can reach more 92% in flood of January 1988 (Table 9).

The comparison of the estimated eroded sediment rate from the RUSLE to the suspended sediment yield from the gauging station shows that more than 68% of the eroded sediments are deposited during the runoff to the outlet of Wadi El Maleh watershed. This value is different from those obtained in many semi-arid watersheds in Algeria (Benchettouh et al. 2017; Hallouz et al. 2017; Djoukbala et al. 2018). This outcome can be explained by the low slope and by the dense vegetation cover of Wadi El Maleh watershed.

Conclusion

The purpose of this work was to assess the spatialization of water erosion risk in Wadi El Maleh watershed in north-western of Algeria, using the very widespread model of RUSLE equation under GIS techniques. It appears in this study that the water erosion is omnipresent in the whole watershed area, with a variable rate. The specific erosion varies from 0 to 754 t/ha/year over the entire study area, with an average of annual soil loss about 9 t/ha/year.

It can also observed that the soil loss varies according to the rainfall erosivity and the vegetation density. The higher the values of erosivity R and the land use C , the more the land is predisposed to water erosion.

A low rate of the eroded sediments reached the outlet of the watershed by runoff; it is estimated from the data of the gauging station, at only, 2.94 t/ha/year, about 32.6% of the total eroded sediment rate quantified by the RUSLE. This value is different from those obtained in many semi-arid watersheds in Algeria. This difference is due to the low slope and the dense vegetation cover of Wadi El Maleh watershed.

RUSLE has proved to be a simple and practical model in this context. It allows to analyze the evolution of soil erosion in a complete and systematic way and provide a reference basis for soil and water loss prevention in this region, and to provide significant information which can assist decision-makers in formulating more effective soil and water conservation plans for the Wadi El Maleh watershed in the future, this method provides an important support to farmers for the identification of areas requiring the highest priority of preventive intervention for the soil conservation.

Publisher's Note Springer Nature remains neutral with regard to jurisdictional claims in published maps and institutional affiliations.

References

- Achite M., & Meddi M. (2004). Estimation du transport solide dans le bassin-versant de l'oued Haddad (Nord-Ouest algérien). *Science et changements planétaires / Sécheresse* 15:367–373.
- Anache, J. A. A., Bacchi, C. G. V., Panachuki, E., & Alves Sobrinho, T. (2015). Assessment of methods for predicting soil erodibility in soil loss modeling. *Geociências*, 34, 32–40.
- Angima, S. D., Stott, D. E., O'Neill, M. K., Ong, C. K., & Weesies, G. A. (2003). Soil erosion prediction using RUSLE for central Kenyan highland conditions. *Agriculture, Ecosystems and Environment*, 97, 295–308. [https://doi.org/10.1016/S0167-8809\(03\)00011-2](https://doi.org/10.1016/S0167-8809(03)00011-2).
- Arnoldus, H.M.J. (1980). Methodology used to determine the maximum potential average soil loss due to sheet and rill erosion in Morocco, Bulletin F.A.O. 34.
- Benchettouh, A., Kouri, L., & Jebari, S. (2017). Spatial estimation of soil erosion risk using RUSLE/GIS techniques and practices conservation suggested for reducing soil erosion in Wadi Mina watershed (northwest, Algeria). *Arabian Journal of Geosciences*, 10. <https://doi.org/10.1007/s12517-017-2875-6>.
- Bouguerra, H., Bouanani, A., Khanchoul, K., Derdous, O., & Tachi, S. E. (2017). Mapping erosion prone areas in the Bouhamdane watershed (Algeria) using the revised universal soil loss equation through GIS. *Journal of Water and Land Development*, 32, 13–23. <https://doi.org/10.1515/jwld-2017-0002>.
- Chadli, K. (2016). Estimation of soil loss using RUSLE model for Sebou watershed (Morocco). *Modeling Earth Systems and Environment*, 2, 51. <https://doi.org/10.1007/s40808-016-0105-y>.
- Djoukbal, O., Mazour, M., Hasbaia, M., & Benselama, O. (2018). Estimating of water erosion in semiarid regions using RUSLE equation under GIS environment. *Environmental Earth Sciences*, 77(9). <https://doi.org/10.1007/s12665-018-7532-1>.
- Duarte, L., Teodoro, A. C., Gonçalves, J. A., et al. (2016). Assessing soil erosion risk using RUSLE through a GIS open source desktop and web application. *Environmental Monitoring and Assessment*, 188. <https://doi.org/10.1007/s10661-016-5349-5>.
- Elaloui, A., Marrakchi, C., Fekri, A., Maimouni, S., & Aradi, M. (2017). USLE-based assessment of soil erosion by water in the watershed upstream Tessaout (Central High Atlas, Morocco). *Modeling Earth Systems and Environment*, 1–13. <https://doi.org/10.1007/s40808-017-0340-x>.
- Fao, I., Rome, I.I. (2012). Harmonized World Soil Database, FAO, Rome., FAO, Rome, Italy and IIASA, Laxenburg, Austria.
- Fernández, C., & Vega, J. A. (2016). Evaluation of RUSLE and PESERA models for predicting soil erosion losses in the first year after wildfire in NW Spain. *Geoderma*, 273, 64–72. <https://doi.org/10.1016/j.geoderma.2016.03.016>.
- Foster, G. R., Toy, T. E., & Renard, K. (2003). Comparison of the USLE, RUSLE1.06c, and RUSLE2 for application to highly disturbed lands. In *First Interagency Conference on Research in Watersheds, October 27–30* (pp. 154–160). Washington, DC: United States Department of Agriculture.
- Ganasri, B. P., & Ramesh, H. (2016). Assessment of soil erosion by RUSLE model using remote sensing and GIS—a case study of Nethravathi Basin. *Geoscience Frontiers*, 7, 953–961.
- Gitas, I. Z., Douros, K., Minakou, C., & Silleos, G. N. (2009). Multi-temporal soil erosion risk assessment in N. Chalkidiki using a modified USLE raster model. *EARSeL eProceedings*, 8, 40–52.
- Hallouf, F., Meddi, M., & Mahe, G. (2017). Régimes des matières en suspension dans le bassin versant de l'oued Mina sur l'oued Cheliff (Nord-Ouest Algérien). *Houille Blanche*, 61–71. <https://doi.org/10.1051/lhb/2017034>.
- Hasbaia, M., Dougha, M., & Benjedou, F. (2017). Erosion sensitivity mapping using a multi-criteria approach under GIS environment the case of the semiarid Hodna Basin in Central Algeria. *International Journal of Water Resources and Arid Environments*, 6(1), 13–19.
- Kalman, R. (1967). Le facteur climatique de l'érosion dans le bassin de Sebou. *Projet Sebou, Rapp. Inédit*, p. 40.
- Karamesouti, M., Petropoulos, G. P., Papanikolaou, I. D., Kairis, O., & Kosmas, K. (2016). Erosion rate predictions from PESERA and RUSLE at a Mediterranean site before and after a wildfire: Comparison & implications. *Geoderma*, 261, 44–58. <https://doi.org/10.1016/j.geoderma.2015.06.025>.
- Khosrowpanah, S., Heitz, L., Wen, Y., & Park, M. (2007). *Developing a GIS-based soil erosion potential model of the UGUM watershed. Technical Report, no. 117*. Mangilao: Water and Environmental Research Institute, University of GUAM.
- Kumar, S., & Gupta, S. (2016). Geospatial approach in mapping soil erodibility using CartoDEM—A case study in hilly watershed of lower Himalayan range. *Journal of Earth System Science*, 125(7), 1463–1472.
- MADR. (2011). *Rapport du Ministère de l'Agriculture et du Développement rural*. p. 85.
- Markose, V. J., & Jayappa, K.S. (2016). Soil loss estimation and prioritization of sub-watersheds of Kali River basin, Karnataka, India, using RUSLE and GIS. *Environmental*

- Monitoring and Assessment*, 188. <https://doi.org/10.1007/s10661-016-5218-2>.
- Mazour, M. (1991). Les facteurs de risque de l'érosion en nappe dans le bassin versant d'isser Tlemcen Algérie, communication n 8, Grenoble, pp. 300–313.
- Mazour, M., Roose, E. (2002). Influence de la couverture végétale sur le ruissellement et l'érosion des sols sur parcelles d'érosion dans des bassins versants du Nord-Ouest de l'Algérie, pp. 320–330.
- McCool, D. K., Foster, G. R., Renard, K., Yoder, D. C., & Weesies, G. A. (1995). The revised universal soil loss equation, Department of Defense/Interagency Workshop on Technologies to Address Soil Erosion on Department of Defense Lands San Antonio, TX, June 11–15.
- Neitsch, S., Arnold, J., Kiniry, J., & Williams, J. (2011). Soil & water assessment tool theoretical documentation version 2009. *Texas Water Resources Institute*, 1–647. <https://doi.org/10.1016/j.scitotenv.2015.11.063>.
- Ozsoy, G., & Aksoy, E. (2015). Estimation of soil erosion risk within an important agricultural sub-watershed in Bursa, Turkey, in relation to rapid urbanization. *Environmental Monitoring and Assessment*, 187, 1–14. <https://doi.org/10.1007/s10661-015-4653-9>.
- Rango, A., & Arnoldus H.M.J. (1987). Aménagement des bassins versants (Watershed management). Cahiers techniques de la FAO, pp. 1–11.
- Rejani, R., Rao, K. V., Osman, M., Srinivasa Rao, C., Reddy, K. S., Chary, G. R., Pushpanjali, & Samuel, J. (2016). Spatial and temporal estimation of soil loss for the sustainable management of a wet semi-arid watershed cluster. *Environmental Monitoring and Assessment*, 188, 1–16. <https://doi.org/10.1007/s10661-016-5143-4>.
- Roose, E. J., & Lelong, F. (1976). Les facteurs de l'érosion hydrique en Afrique tropicale, étude sur petites parcelles expérimentales de sol. *Revue de Géographie Physique et de Géologie Dynamique*, XVIII(4), 365–374.
- Ryan, J. (1982). *A perspective on soil erosion and conservation in Lebanon* (publication n° 69, p. 68). Beyrouth: American University of Beirut.
- Sadiki, A., Bouhlassa, S., Auajjar, J., Faleh, A., & Macair, J. J. (2004). Utilisation d'un SIG pour l'évaluation et la cartographie des risques d'érosion par l'Equation universelle des pertes en sol dans le Rif oriental (Maroc) : cas du bassin versant de l'oued Boussouab. *Bulletin de l'Institut Scientifique, Rabat, section Sciences de la Terre*, 26, 69–79. <https://doi.org/10.19044/esj.2016.v12n32p277>.
- Semwal, P., Khobragade, S. D., & Nainwal, H. C. (2017). Modelling of recent Erosion rates in a Lake catchment in the North-Western Siwalik Himalayas. *Environmental Processes*, 4, 355–374. <https://doi.org/10.1007/s40710-017-0234-y>.
- Siciliano, G. (2009). Social multicriteria evaluation of farming practices in the presence of soil degradation. A case study in southern Tuscany, Italy. *Environment, Development and Sustainability*, 11, 1107–1133. <https://doi.org/10.1007/s10668-008-9169-9>.
- Tahiri, M., Tabyaoui, H., Tahiri, A., El Hadi, A., El Hammichi, F., & Achab, M. (2016). Modelling soil Erosion and sedimentation in the Oued Haricha Sub-Basin (Tahaddart Watershed, Western Rif, Morocco): risk assessment. *Journal of Geoscience and Environment Protection*, 4, 107–119. <https://doi.org/10.4236/gep.2016.41013>.
- Toubal, A. K., Achite, M., Ouillon, S., & Dehni, A. (2018). Soil erodibility mapping using the RUSLE model to prioritize erosion control in the Wadi Sahouat basin, north-west of Algeria. *Environmental Monitoring and Assessment*, 190, 210. <https://doi.org/10.1007/s10661-018-6580-z>.
- Toumi, S., Meddi, M., Mahé, G., & Brou, Y. T. (2013). Cartographie de l'érosion dans le bassin versant de l'Oued Mina en Algérie par télédétection et SIG. *Hydrological Sciences Journal*, 58, 1542–1558. <https://doi.org/10.1080/02626667.2013.824088>.
- Vezena, K., & Bonn, F. (2006). Modélisation et analyse de la dynamique spatio-temporelle des relations société-érosion et pollution diffuse en milieu agricole. Etude de cas en Vietnam et au Québec. Interaction Nature-Société, analyse et modèles. UMR6554 LETG, La Baule.
- Wall, G. J., Coote, D. R., Pringle, E. A., & Shelton, I. J. (2002). Revised universal soil loss equation for application in Canada: a handbook for estimating soil loss from water erosion in Canada. *Agriculture and Agri-Food Canada*. Res. Branch Ott. Contrib. No AAFCAAC2244E.
- Warwade, P., Hardaha, M. K., & Kumar, D. (2014). Estimation of soil erosion and crop suitability for a watershed through remote sensing and GIS approach. *Indian Journal of Agricultural Sciences*, 84, 18–23.
- Wawer, R., Nowocien, E., & Podolski, B. (2005). Real and calculated K USLE erodibility factor for selected polish soils. *Polish Journal of Environmental Studies*, 14(5), 655–658.
- White, W.R. (1986). Problèmes d'érosion, transport solide et sédimentation dans les bassins versants, Projet 5.3 du programme hydrologique international. Paris: UNESCO, Etudes et rapports d'hydrologie no. 35. http://hydrologie.org/BIB/Publ_UNESCO/SR_035_F_1986.pdf. [accédé le 8 juillet 2013].
- Williams, J. R. (1975). Sediment routing for agricultural watersheds. *Water Resources Bulletin*, 11(5), 965–974.
- Williams, J. R., & Berndt, H. D. (1977). Sediment yield prediction based on watershed hydrology. *Transactions of the American Society of Agricultural and Biological Engineers [online]*, 20(6), 1100–1104. <https://doi.org/10.13031/2013.35710>.
- Wischmeier, W. H., & Smith, D. D. (1965). Predicting rainfall erosion losses from cropland east of the Rocky Mountains [online]. In *Agricultural Handbook 282* (p. 47). Brooksville: US Department of Agriculture - Agricultural Research Service.
- Wischmeier, W. H., & Smith, D. D. (1978). Predicting rainfall erosion losses - a guide to conservation planning. In *Agriculture Handbook No 537*. Washington, DC: U.S. Department of Agriculture.